Molecular and macroscopic orientational order in aramid solutions: a model to explain the influence of some spinning parameters on the modulus of aramid yarns

S. J. Picken, S. van der Zwaag and M. G. Northolt
Akzo Research Laboratories Arnhem, Corporate Research, Physical Chemistry Department, PO Box 9300, 6800 SB Arnhem, The Netherlands
(Received 1 May 1991; revised 6 June 1991; accepted 24 July 1991)

A semi-empirical model is presented for the calculation of the overall orientation in nematic aramid solutions during the fibre spinning process. The model describes the effect of coagulation-bath temperature, polymer concentration, and draw ratio on the modulus of poly(*p*-phenylene terephthalamide) yarns. The results of the model are compared with experimental results for the E modulus of as-spun aramid fibres.

(Keywords: PpPTA; fibre spinning; lyotropic solutions; modulus; affine deformation; mean-field model)

INTRODUCTION

Sulphuric acid solutions of the fully aromatic polyamide (or aramid) PPTA are used to produce high-modulus, high-tenacity fibres. *Figure 1* shows the aramid polymers poly(*p*-phenylene terephthalamide) (PPTA) and poly(4,4′-benzanilidylene terephthalamide) (DABT). These polymers form a lyotropic nematic phase between about 8 and 20 wt% polymer concentration in concentrated ($\geqslant$99.8%) H_2SO_4. At $\approx$20 wt% the solubility limit is reached. The DABT polymer is used for experimental purposes, as it has the advantage that it does not form a crystal–solvate phase at room temperature, even for the highest concentration.

Figure 2 shows schematically an experimental set-up for the dry-jet wet spinning process. The aramid solution is extruded through the spinneret and stretched in the air gap above the coagulation bath. In the coagulation bath the sulphuric acid is removed and the aramid fibre is formed. In the arrangement shown, the winding tension can be adjusted separately.

For fibre spinning, usually a concentrated solution of PPTA of $\approx$19.6 wt% is used. The temperature of the solution is $\approx$80°C. In such solutions a high degree of molecular orientation of the polymer chains with respect to the local director can be expected. This orientation of the polymer chains with respect to the local director is modelled here using a theory analogous to the Maier–Saupe model for low-molecular-weight nematics[1,2].

During the spinning process the local directors are aligned in the direction of flow by the shear flow in the capillaries of the spinneret and by the elongational flow in the entrance zone above the spinneret and in the air gap. The high degree of orientation of the director thus obtained, together with the high degree of local molecular (orientational) order, implies that the polymer chains are highly oriented in the direction of flow. Assuming that this orientational order is merely 'frozen-in' during the coagulation process, the high modulus of the aramid fibre obtained can be predicted quantitatively using some simple models for the molecular orientation in the lyotropic liquid-crystalline solution.

In the following, the mean-field model for the orientational order with respect to the director is briefly reviewed. To describe the degree of director orientation due to the flow history, an affine deformation model is used. Finally, a model predicting the modulus of aramid yarns from the average crystallite orientation[3] is used to make the connection from molecular order to mechanical yarn properties. Experimental results on the yarn modulus are compared with this simple model as a function of polymer concentration, draw ratio in the air gap, and coagulation bath temperature.

It is noted that this approach is not intended to provide a complete constitutive equation to describe the flow behaviour of a lyotropic nematic main-chain polymer solution; such an approach has been provided by the theory of Doi and Edwards[4], with some recent additional contributions by Marucci[5] and Larson[6]. The present approach is essentially a semi-empirical one where the various parts of the model are justified by the surprisingly good agreement with experimental results.

MEAN-FIELD MODEL FOR LOCAL ORIENTATIONAL ORDER

In previous publications[1,2] a mean-field model analogous to the Maier–Saupe model for low-molecular-weight nematics[7] was used to describe the local molecular orientational order in a lyotropic polymeric system. Here this model is briefly reviewed and some useful asymptotic relations for the high orientational order limit

0032-3861/92/142998-09

PPTA

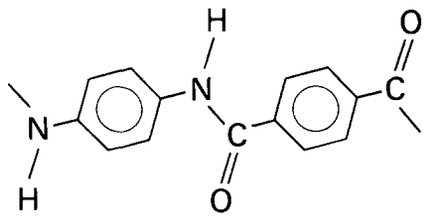

DABT

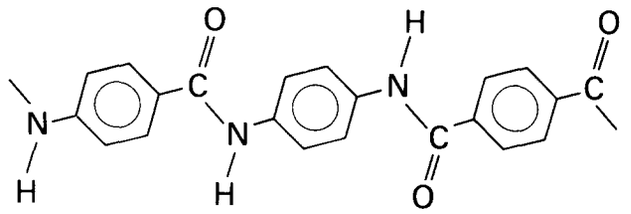

Figure 1 The aramid polymers poly(*p*-phenylene terephthalamide) (PPTA) and poly(4,4'-benzanilidylene terephthalamide) (DABT)

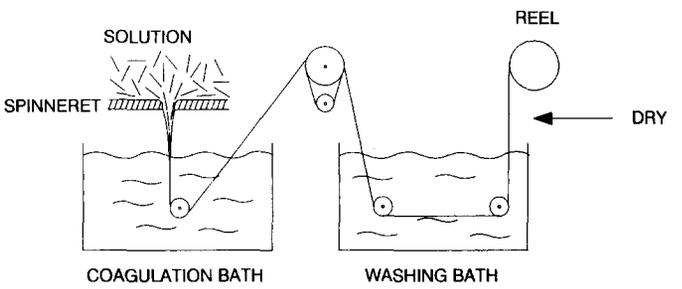

Figure 2 Schematic drawing of the aramid fibre spinning process

are given. The model allows the prediction of the molecular degree of orientational order with respect to the (local) director, as shown in *Figure 3*, where β is the angle of the polymer chain tangent with respect to the director.

In the well-known Maier–Saupe model for low-molecular-weight nematics, use is made of an effective mean-field potential of the form

$$U = -\varepsilon \langle P_2 \rangle P_2(\cos\beta) \qquad (1)$$

where $P_2(\cos\beta) = \frac{1}{2}(3\cos^2\beta - 1)$ is the second-order Legendre polynomial of $\cos\beta$, and $\langle P_2 \rangle$ is the average of $P_2(\cos\beta)$ taken over the molecular orientational distribution function $f(\beta)$, i.e.

$$\langle P_2 \rangle = \int_{-1}^{1} \mathrm{d}(\cos\beta)\, f(\beta) P_2(\cos\beta) \qquad (2)$$

The value of $\langle P_2 \rangle$ is 0 for an isotropic phase and 1 for perfect orientational order along the director.

In a nematic phase the orientational distribution has a maximum at angles $\beta = 0$ and $\beta = \pi$. The distribution function using Boltzmann statistics is given by

$$f(\beta) = \frac{1}{Z}\exp\left(\frac{-U}{kT}\right) = \frac{1}{Z}\exp\left[\frac{\varepsilon}{kT}\langle P_2 \rangle P_2(\cos\beta)\right] \qquad (3)$$

where Z is the partition function, given by

$$Z = \int_{-1}^{1} \mathrm{d}(\cos\beta)\exp\left[\frac{\varepsilon}{kT}\langle P_2 \rangle P_2(\cos\beta)\right] \qquad (4)$$

Substituting equations (3) and (4) into equation (2) leads to a self-consistent equation for $\langle P_2 \rangle$ as a function of kT/ε, the reduced temperature. For all temperatures, $\langle P_2 \rangle = 0$ (the isotropic phase) is a possible solution to this equation. However, by demanding that the free energy should be minimal, a first-order phase transition is found to a solution with $\langle P_2 \rangle = 0.38$ at $kT/\varepsilon = 0.22$. Further reduction of the temperature leads to an increase in $\langle P_2 \rangle$; see *Figure 4*. For temperatures well below T_{ni}, the order parameter $\langle P_2 \rangle$ in the Maier–Saupe model is given approximately by

$$\langle P_2 \rangle \approx 1 - \frac{kT}{\varepsilon} \qquad (5)$$

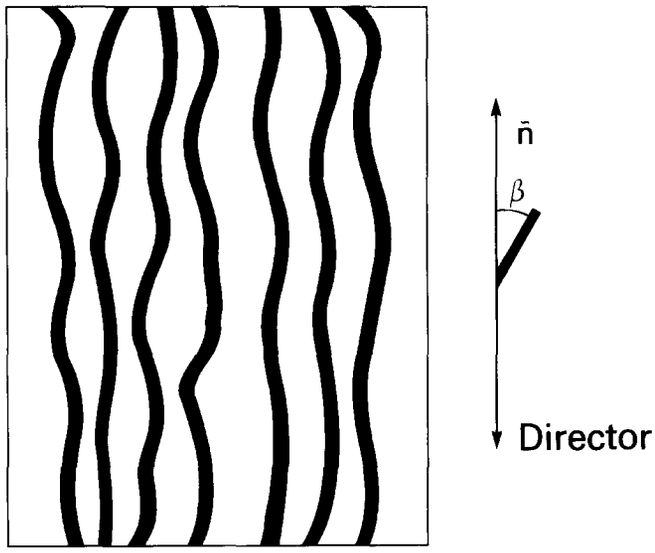

Figure 3 Local orientational order in the nematic phase of worm-like polymer chains, showing the angle β with respect to the director $\tilde{n}$

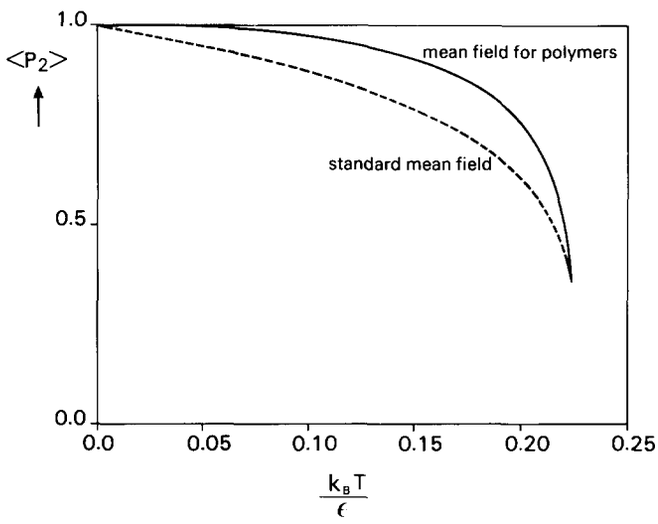

Figure 4 Theoretical curves of the $\langle P_2 \rangle$ order parameter as a function of the 'reduced temperature' kT/ε. (– – –), Standard Maier–Saupe mean-field theory; (——), adapted mean-field theory for polymers, with the position of the phase transition scaled to coincide with the standard theory for easy comparison

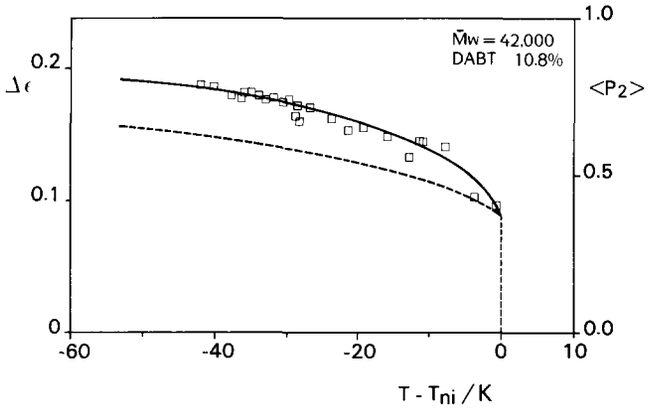

Figure 5 Experimental values (□) of the dielectric anisotropy (for optical frequencies) as a function of temperature for a 10.8 wt% DABT solution, $M_w = 42000$. (– – –), Standard Maier–Saupe theory; (——) mean-field theory for polymers described in the text

To extend the standard model given above to the case of lyotropic polymers, the effects of molecular flexibility and polymer concentration are included in the strength of the potential ε, using

$$\varepsilon = \varepsilon^* c^2 L^2(T) \tag{6}$$

where ε^* is a constant determining the absolute temperature scale, c is the concentration of the polymer in the solution, and $L(T)$ is the temperature-dependent 'contour projection length', which is the average length of the projection of the worm-like polymer chain along the direction of the first segment. For rod-like polymer chains, $L(T)$ is just the end-to-end distance L_c or the contour length. For coil-like polymer chains, $L(T)$ is equal to the persistence length L_p. Using a simple potential of the form

$$U_c = A \cos\theta \tag{7}$$

to describe the bending energy of the worm-like chains, where θ is the angle between subsequent 'segments' of the chain, and taking the continuous limit, the contour projection length $L(T)$ is given by[1,2]

$$L(T) = L_p \frac{1 - \exp(-L_c T / L_p T_p)}{T/T_p} \tag{8}$$

Here L_c is the contour length and L_p is the persistence length at temperature T_p. Usually T_p will be room temperature, depending on the conditions used to measure L_p. Observe that indeed for low contour length and/or low temperature, $L(T) = L_c$ and that for high temperature and/or high contour length, equation (8) reduces to

$$L(T) \approx L_p T_p / T \tag{9}$$

i.e. the persistence length at temperature T. Note that the persistence length is inversely proportional to the absolute temperature. This is a consequence of the use of a potential to describe the bending of the worm-like chain, equation (7).

By substituting equations (6) and (8) into the standard Maier–Saupe model, $\langle P_2 \rangle$ can be calculated as a function of polymer concentration and temperature. *Figure 4* shows the result for a high contour length L_c (the continuous curve). The ordinate is scaled to allow comparison with standard Maier–Saupe theory. It is observed that $\langle P_2 \rangle$ increases more rapidly for polymer chains with decreasing temperature, due to the effect of chain-stiffening (the persistence length increases). In *Figure 5* the models are compared with experimental results for the anisotropy of the dielectric constant $\Delta\varepsilon$ (at optical frequencies), which is proportional to $\langle P_2 \rangle$:

$$\Delta\varepsilon = \Delta\varepsilon_0 \langle P_2 \rangle \tag{10}$$

The unknown constant $\Delta\varepsilon_0$ is the anisotropy that would be found in the case of perfect molecular orientation. The results in *Figure 5* were obtained by measuring the birefringence of an aramid solution with an Abbe refractometer; for further details see ref. 2.

Good agreement is observed with the authors' model that includes the effect of temperature-dependent chain flexibility. However, the scatter in the experimental results does not allow an unambiguous choice between the two mean-field models to be made, due to the fact that the exact value of $\Delta\varepsilon_0$ is unknown.

The combined effects of polymer concentration and molecular weight are demonstrated in *Figure 6* where experimental and theoretical results for the nematic–isotropic transition temperature (the clearing temperature) are shown. The values of clearing temperature were obtained using a polarizing microscope and a hot stage. The values for T_{ni} shown are at 50% phase separation; the biphasic gap was $\approx 5°C$.

Of course, the absolute temperature scale has to be determined from the experimental results. For this purpose the filled point in *Figure 6* (at $c = 11$ wt%, $T_{ni} = 98°C$) was used for the calculation of ε^*:

$$\varepsilon^* = \frac{kT_{ni}}{0.22 L^2(T_{ni}) c^2} \tag{11}$$

This equation is immediately obtained by combining equation (6) with the value of $kT/\varepsilon = 0.22$ at the phase transition. Equation (11), now that the value of ε^* is known, is used to calculate the influence of concentration and molecular weight on the clearing temperature T_{ni}. The curves drawn in *Figure 6* represent the theory; good agreement with the experimental results is observed. Both the influence of concentration and that of molecular weight on the clearing temperature are described adequately by this model. A single value of the parameter ε^* is used for both curves. The influence of molecular

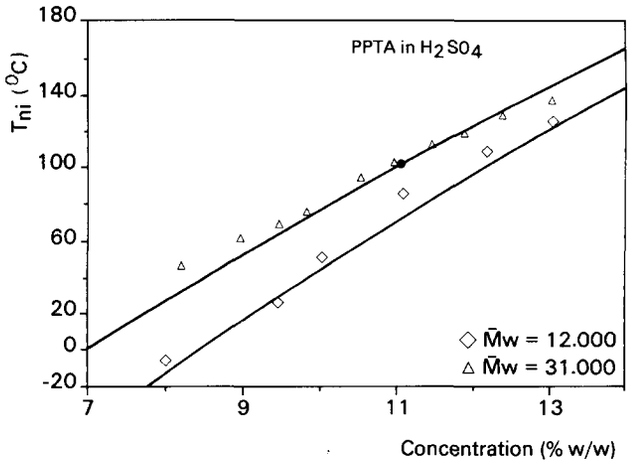

Figure 6 Experimental values (△, ◇) of clearing temperature T_{ni} of two PPTA samples as a function of polymer concentration. (●), Data point used to determine ε^* (see text); (——) modified mean-field theory for lyotropic polymers

weight is taken into account via the contour length L_c in equation (8). We used M_w values obtained from an empirical calibration curve to calculate L_c.

In the following the temperature and concentration dependence of $\langle P_2 \rangle$ as given by our model is used to predict the molecular degree of orientation during the spinning process.

For practical purposes it is often convenient to use some approximate relations for T_{ni} and $\langle P_2 \rangle$. Equation (11) may be written as

$$T_{ni} \approx Ac^{\alpha} \tag{12a}$$

where $A = 76$ K, c is in wt%, and $\alpha = 0.66$. From equations (5), (9) and (11), we find

$$\langle P_2 \rangle \approx 1 - 0.22(T/T_{ni})^3 \tag{12b}$$

The value of 0.66 for α in equation (12a) is obtained if the influence of contour length is disregarded in equation (8). For standard solutions with a contour length $L_c \approx 150$ nm this is a good approximation. The value for A in equation (12a) is derived from the fit with the experimental data in *Figure 6* (the filled point). The T^3 term in equation (12b) is due to the $L^2(T)$ term in equation (6) combined with the linear term in T in equation (5). Note that equation (12b) is valid only in the limit of high orientational order, i.e. for temperatures well below T_{ni} and for sufficiently high molecular weights. In aramid fibre spinning experiments these requirements are usually fulfilled. The extrapolated value of T_{ni} at a concentration of 19.8 wt% is ≈ 545 K, while the spinning temperature is around 350 K. The contour length L_c is on average about five times L_p, so the exponential term in equation (8) can be ignored.

AFFINE DEFORMATION MODEL FOR AVERAGE DIRECTOR ORIENTATION

In this section a model is introduced that allows the calculation of the degree of director orientation as a function of external flow fields. First some experimental results on the orientation of lyotropic DABT solutions in H_2SO_4 using a simple shear geometry will be discussed. The experimental results for simple shear can be described by an affine deformation model, which is then also used for elongational flow, to allow the calculation of the director orientation during fibre spinning.

In a previous publication[8], results were presented from synchrotron X-ray scattering on DABT solutions during simple shear flow. The measured 'order parameter' S_{exp} is the average of $P_2(\cos\beta)$ over the experimental orientational distribution of the 003 meridional reflection.

The experimental 'order parameter' S_{exp} is influenced by (1) the degree of local molecular order with respect to the director, (2) the degree of director orientation, and (3) the degree of lateral correlation between the polymer chains. This is described by the equation

$$S_{exp} = K\overline{P_2}\langle P_2 \rangle \tag{13}$$

Here the local molecular orientational order is given by $\langle P_2 \rangle$ and the macroscopic director orientation is given by $\overline{P_2}$. The additional azimuthal broadening due to lateral correlation is described by K. This factor K can be imagined to be the apparent order parameter that would be found for a sample with perfect orientational order in which the meridional reflections are still broadened by the lateral disorder along the molecular c-axis[9].

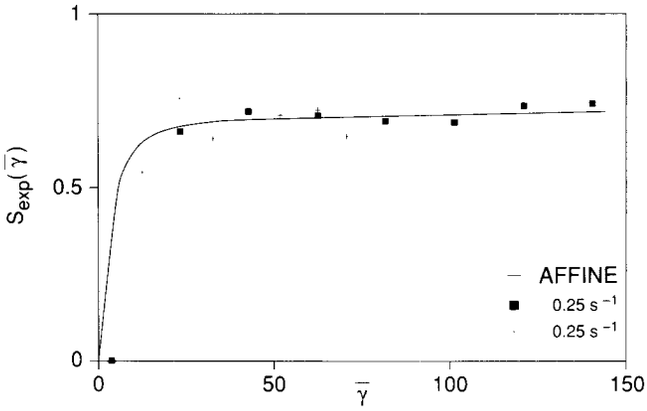

Figure 7 Experimental order parameter S_{exp} from synchrotron X-ray scattering as a function of shear strain γ for a shear rate of 0.25 s^{-1}. (■, +) Different experiments on the same DABT solution, 20 wt%, $M_w = 30000$, 20°C, showing the experimental scatter of the data; (——) simple-shear affine deformation model

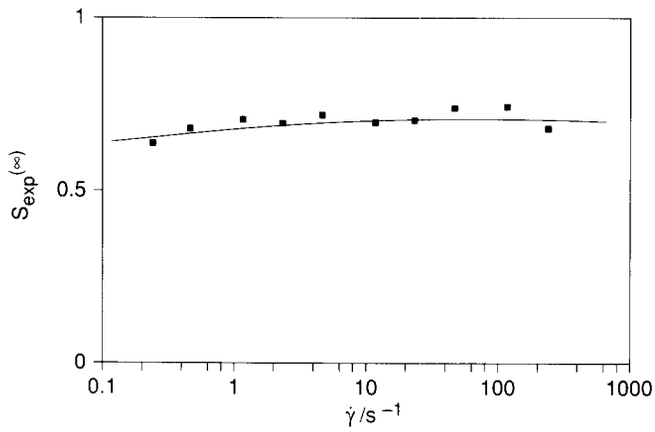

Figure 8 Steady-state experimental order parameter S_{exp} from synchrotron X-ray scattering as a function of shear rate $\dot{\gamma}$, using the same DABT sample as for *Figure 7*

It is now assumed that the product $K\langle P_2 \rangle$ is a local molecular property that is independent of external flow fields. Equation (13) shows that S_{exp} and $\overline{P_2}$ are then proportional. By measuring S_{exp} it is possible to derive information on $\overline{P_2}$.

Figure 7 shows the development of S_{exp} as a function of shear strain γ for a shear rate $\dot{\gamma}$ of 0.25 s^{-1}. The experimental orientation S_{exp} increases with γ, levelling off to a value of about 0.75. *Figure 8* shows the steady-state results for S_{exp} (i.e. for large applied strains γ) as a function of shear rate $\dot{\gamma}$. It appears that the ultimate large strain value of S_{exp} is more or less independent of $\dot{\gamma}$. As it is known from e.g. polarization microscopy that at high shear rates the director is fully aligned along the direction of flow (i.e. $\overline{P_2} = 1$), it is concluded from *Figure 8* that the value of $K\langle P_2 \rangle$ is ≈ 0.73. This level for S_{exp} apparently corresponds to the case $\overline{P_2} = 1$. It can be estimated from the mean-field model in the previous section that $\langle P_2 \rangle$ should be ≈ 0.96 (using 20°C, 20 wt%). This means that the value of K is ≈ 0.77, so broadening of the meridional reflections due to lateral disorder of the polymer chains appears to be an important factor. This value of K is in reasonable agreement with an estimate obtained by visually comparing the azimuthal half-widths of meridional and

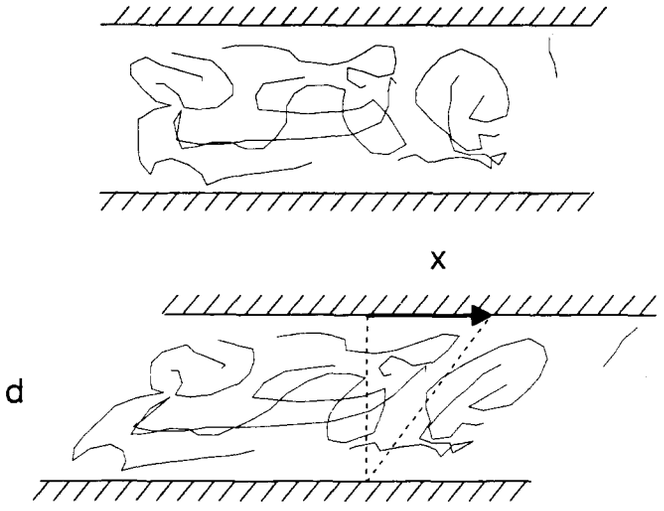

Figure 9 Affine simple-shear deformation computed for a shear strain $\gamma = x/d$, indicating how a random director field is oriented and stretched due to the application of an affine simple shear deformation

equatorial reflections: $K = 0.82 \pm 0.05$. The curve drawn in *Figure 7* shows the development of the director order $\overline{P_2}$ as a function of γ from an affine simple-shear deformation model. Reasonable agreement is observed with the experimental results.

Deformation models in which the sample is deformed uniformly according to the macroscopic deformation of the sample are referred to as affine models. The effect of an affine deformation in simple shear on the director field is shown schematically in *Figure 9*. All coordinates are transformed as prescribed by the overall deformation tensor of the sample:

$$\begin{bmatrix} x \\ y \\ z \end{bmatrix}' = \begin{bmatrix} 1 & 0 & 0 \\ 0 & 1 & 0 \\ \gamma & 0 & 1 \end{bmatrix} \begin{bmatrix} x \\ y \\ z \end{bmatrix} \tag{14}$$

Using a numerical model it is possible to calculate the average director orientation as a function of shear strain γ; see *Figure 10*.

The numerical method consists in taking a unit vector from an isotropic director distribution, transforming it according to equation (14) and subsequently calculating the $P_2(\cos\theta)$ value (where θ is defined with respect to the direction of flow along the z-axis). This process is repeated until sufficient accuracy for $\overline{P_2}$ has been obtained, e.g. 1000 times for each strain value γ. For more details see ref. 8 or 10.

Apart from $\overline{P_2}$ with respect to the direction of flow, *Figure 10* also shows $\overline{D}$ (the average of $3\sin^2\theta\cos(2\varphi)/2$, where θ is the angle with respect to the z-axis and φ is the azimuthal angle with respect to the x-axis), the macroscopic 'flatness order parameter'. That $\overline{D}$ is not zero indicates that the director orientation distribution is not completely axially symmetric. This also means that equation (13) is an approximation, as the influence of $\overline{D}$ is not taken into account. It is noted however that the value of $\overline{D}$ remains small, so this will not lead to a serious error. The numerical results for $\overline{P_2}$ and $\overline{D}$ can be approximated by the following analytic expressions:

$$\overline{P_2}(\gamma) = \left[1 - \frac{3\gamma}{2\gamma^2 + 90}\right]\left[\frac{\gamma^2}{\gamma^2 + 6}\right] \tag{15a}$$

$$\overline{D}(\gamma) = \frac{\gamma(1 - e^{-3/2\gamma})}{\gamma + 10(1 - e^{-3/2\gamma})} \tag{15b}$$

These expressions were obtained by analysing the asymptotic behaviour of the numerical results and then using a trial-and-error method. Equations (15a,b) are also shown in *Figure 10* (dashed lines) to demonstrate the good agreement with the numerical results.

For modelling the spinning process, the equivalent of this affine deformation model for simple shear is used, but now for elongational flow. Unlike the case of simple shear, the calculation can be done analytically leading to the Kuhn and Grün equation[11]:

$$\overline{P_2(a)} = \frac{2a^3 + 1}{2(a^3 - 1)} - \frac{3a^3}{2(a^3 - 1)^{3/2}} \operatorname{atan}\{(a^3 - 1)^{1/2}\} \tag{16}$$

where $a = 1 + \gamma$ is the degree of elongation (i.e. $x' = x/\sqrt{a}$, $y' = y/\sqrt{a}$, and $z' = za$). Of course, in this case $\overline{D} = 0$, from symmetry arguments. The Kuhn and Grün equation was originally derived for the change in orientational order in an ideal rubber due to elongation. Of course, exactly the same result is obtained if uniaxial elongation instead of simple shear is used in equation (14). This was used to test the computer program.

The result for elongation is also shown in *Figure 10* by the continuous curve. It is of interest to study the asymptotic behaviour of equations (15a) and (16) for large strains:

simple shear:

$$\overline{P_2(\gamma)} = 1 - \frac{3}{2\gamma} \tag{17a}$$

elongation:

$$\overline{P_2(\gamma)} = 1 - \frac{3\pi}{4\gamma^{3/2}} \tag{17b}$$

Note the higher exponent for γ in the case of elongation, which is caused by the radial contraction ($1/\sqrt{a}$). The difference in the exponents explains the general observation that elongational flow is more efficient than simple shear flow for obtaining a high degree of director orientation and corresponding high anisotropy of the mechanical properties[12].

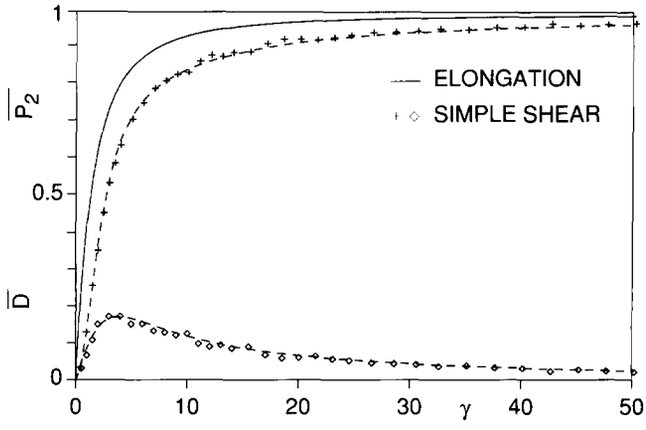

Figure 10 Calculated values of the director order parameters $\overline{P_2}$ (+) and $\overline{D}$ (◇) from simple-shear affine deformation, at shear strain γ (see *Figure 9*). The elongational strain a in equation (16) is $1 + \gamma$. (——), Affine elongation; (– – –) analytic approximations given by equations (15a, b)

OVERALL ORIENTATIONAL ORDER AS A FUNCTION OF TEMPERATURE, POLYMER CONCENTRATION, AND DRAW RATIO

Using the equations describing the molecular and the director order parameters, it is now possible to calculate the overall degree of orientational order as a function of temperature, polymer concentration, and draw ratio. The effects of temperature and concentration are described by the mean-field model. The influence of the draw ratio is described by the Kuhn and Grün equation. The central equation describing the overall orientational order is

$$\overline{\langle P_2 \rangle} = \overline{P_2}\langle P_2 \rangle \tag{18}$$

analogous to equation (13). Note that here the K factor is absent, as the true overall molecular orientation is involved and not the experimentally measured half-width of the meridional 003 reflection that is broadened by the lateral molecular (dis)order. A reasonable estimate for $\langle P_2 \rangle$ as a function of temperature and concentration can be obtained from equations (12a,b). The value of $\overline{P_2}$ as a function of draw ratio can be obtained from equation (16).

For modelling the spinning process, a certain degree of pre-orientation in the solution is postulated, due to the spinneret (i.e. by the entrance zone of the die and the Poiseuille flow in the capillary). To simplify matters, the influence of the entrance zone and the capillary will be described by an 'effective pre-elongation'. No attempt is made to predict the average degree of director orientation due to the spinneret geometry. This semi-empirical approach means that the elongation a in equation (16) is written as

$$a = DR_{\text{pre}} DR_{\text{air-gap}} \tag{19}$$

Here $DR_{\text{air-gap}}$ is the draw-down applied below the spinneret, which can be calculated from the winding speed and the throughput of the spinning pump, and DR_{pre} is the equivalent draw-down that would be required to obtain the same degree of director orientation as that caused by the entrance zone and the capillary of the die.

To analyse the spinning results, E-modulus curves as a function of draw ratio ($DR_{\text{air-gap}}$), polymer concentration, and coagulation bath temperature are fitted to the affine deformation model using two parameters, namely DR_{pre} and $\langle P_2 \rangle$. The DR_{pre} value contains information on the degree of orientation immediately below the capillary in the spinneret. The experimental (fitted) values of $\langle P_2 \rangle$ are compared with the theoretical mean-field results.

The use of equation (19) may be found objectionable, as DR_{pre} is an *ad hoc* correction by which various experimental problems are 'swept under the carpet'. For instance, if there is some slippage compared with the affine model, this will also be absorbed by the DR_{pre} factor. Alternatively, equations (18) and (19) can be regarded as a method of fitting the experimental results so as to obtain a value for $\langle P_2 \rangle$ which can then be compared with the mean-field model.

ORIENTATIONAL ORDER AND FIBRE MODULUS

To calculate the fibre modulus from the overall molecular orientation in the solution, a mechanical model[3] is used. This model provides a relation between the initial E modulus and the average degree of crystallite orientation $\langle \sin^2(\theta) \rangle_{\text{cr}}$ in the fibre:

$$\frac{1}{E} = \frac{1}{e_3} + \frac{\langle \sin^2(\theta) \rangle_{\text{cr}}}{2g} \tag{20}$$

Here E is the fibre modulus, e_3 is the chain modulus ($\approx$240 GPa for PPTA), and g is the shear modulus ($\approx$2 GPa for PPTA). The degree of crystallite orientation can be determined using the azimuthal orientation of the equatorial or the meridional reflections of the fibre X-ray diffraction pattern. In the case of equatorial reflections the factor K, describing the lateral disorder (equation (12)), is 1, due to the crystalline structure of the fibre.

To predict the fibre modulus from the overall degree of orientation in the solution, it is now postulated that the crystallite orientation is given by

$$\langle \sin^2(\theta) \rangle_{\text{cr}} = \tfrac{2}{3}(1 - \overline{\langle P_2 \rangle}) \tag{21}$$

In equation (21) it is assumed that the overall degree of orientation obtained in the fibre is the same as the overall degree of orientation in the solution. This implies that there is no influence of the coagulation process on the overall average degree of orientation. The validity of this approach will be discussed further in the next section.

COMPARISON WITH EXPERIMENTAL RESULTS FROM YARN SPINNING

To test the model described in the previous sections, several spinning experiments were carried out using a small spinning machine. The general principle is shown in *Figure 2*. The coagulation bath temperature, the polymer concentration, and the draw-down in the air gap were varied independently.

The effect of winding tension was also studied, showing an increase in fibre modulus with increasing winding tension. This will not be discussed further here. In order to test the theory, the experimental results for zero winding tension are used. The use of the coagulation bath temperature rather than the spinning temperature (at the spinneret) is motivated by the fact that the exchange of heat with the coagulation bath is a very rapid process. This means that the temperature of the polymer solution during coagulation is determined by the temperature of the coagulation bath.

In *Figure 11* the initial fibre modulus E_i is shown as a function of draw ratio for three polymer concentrations at a constant coagulation bath temperature of 3.6°C. In *Figure 12* the initial fibre modulus E_i is shown as a function of draw ratio for three coagulation bath temperatures at a constant polymer concentration of 19.8 wt%.

Ignoring the scatter in the experimental results, which is caused by the difficulty in maintaining zero winding tension, the curves drawn from the affine deformation model (equations (16), (18) and (19)) describe the results quite well. Deviations of the winding tension always cause an increase in the modulus, so the experimental results with the lowest E modulus are the most reliable.

Table 1 shows the values for DR_{pre} (the 'effective pre-draw') in equation (18) and the values of $\langle P_2 \rangle$ in equation (17) that are used to obtain the curves in *Figures 11* and *12*. The calculated values of $\langle P_2 \rangle$ from the

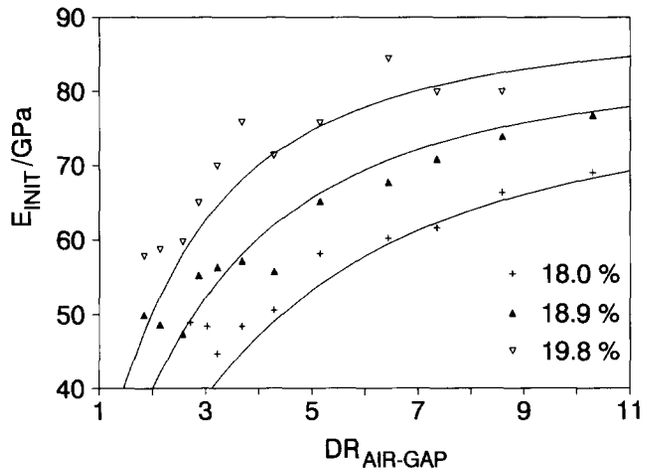

Figure 11 Initial E modulus of PPTA yarns as a function of draw ratio in the air gap for the polymer concentrations shown (wt% in 99.8% H_2SO_4) at a coagulation bath temperature of 3.6°C; DR_{pre} = (▽) 3, (▲) 4.5, (+) 6. (——) Affine deformation model

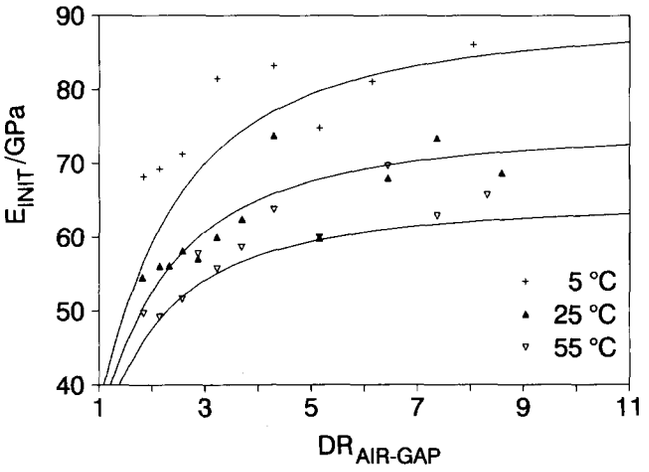

Figure 12 Initial E modulus of PPTA yarns as a function of draw ratio in the air gap for coagulation bath temperatures as shown for a 19.8 wt% PPTA solution in 99.8% H_2SO_4; $DR_{pre} = 8$ in all cases. (——), Affine deformation model

Table 1 Experimentally fitted values of $\langle P_2 \rangle$ and DR_{pre} using the affine deformation model, and the theoretical values of $\langle P_2 \rangle$ from the mean-field model. The $\langle P_2 \rangle$ values are also expressed in terms of a maximum modulus, using equations (20) and (21)

			Experiment		Theory	
c (wt%)	T_{bath} (°C)	DR_{pre}	$\langle P_2 \rangle$	E_{max} (GPa)	$\langle P_2 \rangle$	E_{max} (GPa)
18.0	3.6	3	0.950	80	0.965	100
18.9	3.6	4.5	0.954	85	0.968	106
19.8	3.6	6	0.958	90	0.971	111
19.8	5	8	0.958	90	0.971	110
19.8	25	8	0.945	75	0.963	98
19.8	55	8	0.933	65	0.950	81

mean-field model are also given. These calculated values are from the full numerical treatment; however, it may be shown that equations (12a,b) give nearly the same values of $\langle P_2 \rangle$.

From *Table 1* it is observed that the experimentally determined influences of polymer concentration and coagulation bath temperature are described quite well by the mean-field model. Although the absolute value of the E modulus is not predicted very accurately, it should be realized that the theory has to extrapolate the T_{ni} value to concentrations well above the regime in which experimental data are available. Considering this limitation, it is observed that the variation in the theoretical $\langle P_2 \rangle$ value is in good agreement with the variation in $\langle P_2 \rangle$ obtained by fitting the experimental data to the affine deformation model. Also, the model assumes that the orientational order hardly changes during the coagulation process. From the nearly quantitative agreement with the experimental data for the maximum modulus, this somewhat questionable simplification would seem to be more or less correct. It should also be realized that the E modulus is very sensitive to a slight change in the $\langle P_2 \rangle$ value, so the agreement between theory and experiment is as good as could be hoped for.

Although there is some experimental uncertainty, it is observed that the required amount of pre-elongation DR_{pre} to fit the influence of draw-down increases with increasing polymer concentration. This result suggests that the orientation due to the spinneret is determined not only by geometrical factors, as otherwise DR_{pre} would have been constant. The observed trend in fact suggests a certain degree of slippage, a reduction of the concentration leading to a reduction of DR_{pre}, as would be expected. Note also that for the experiments at different coagulation bath temperatures, only one value for DR_{pre} was used, as is required by the association of DR_{pre} with the orientation due to the spinneret. From the discrepancy between the DR_{pre} value (6) for the highest concentration and the value (8) that seemed to be most appropriate for the whole bath temperature series, it is observed that the fitting process to obtain the maximum modulus or $\langle P_2 \rangle$ is somewhat insensitive to variation of DR_{pre}.

DISCUSSION

The orientation due to elongational flow has been discussed previously by Kenig[13], who used a relation of the form

$$\tan \theta = a^{-p} \tan \theta_0 \qquad (22)$$

where a is the draw ratio and θ is the orientation angle. The exponent p is the 'orientability parameter' that describes to what extent the elongational flow has any effect. For an affine deformation (without slip), p is equal to 3/2. In practice a lower value was reported for a PPTA solution, ≈ 0.6. This result suggested that the orientation process is less efficient than the affine deformation theory predicts.

The apparent contradiction with the present model can be understood if it is realized that in our model orientation angles $\theta = 0$ cannot be reached, because of the limitation that the local molecular order cannot be influenced by external flow fields, i.e. the slow flow regime still operates. The affine deformation model is used only to describe the degree of director orientation. This means that from the present point of view the 'orientability parameter' is another way of expressing the fact that the local molecular order cannot be substantially influenced by the application of an external deformation. This is in agreement with the experimental observation that the

plateau value for the fibre modulus, for high draw ratio, is far lower than the aramid chain modulus of 240 GPa.

In addition, it is noted that for the range of concentrations concerned here, the Doi–Edwards rotational diffusion constant[4] $\bar{D}_r$ (see Appendix) is $\approx 3.3 \times 10^4\ s^{-1}$ if for the effective rod length the persistence length L_p is taken. Any influence of external flow fields on the molecular $\langle P_2 \rangle$ value is expected for deformation rates greater than $\bar{D}_r$ only, i.e. when the so-called dimensionless shear or elongation rate is of the order of 1 or more. The applied shear rate in the spinneret is of this order of magnitude ($\approx 1.5 \times 10^5\ s^{-1}$ at the wall, and $9.2 \times 10^4\ s^{-1}$ on average); however, the applied strain is not very large. The elongation rate in the air gap is well below $\bar{D}_r$, in the region of $600\ s^{-1}$. This means that the shear-induced molecular orientation due to the spinneret (if any) would have enough time to relax to the equilibrium $\langle P_2 \rangle$. For this reason it is felt that the present 'slow flow' approach is justified for the spinning conditions used.

It is noted that this theoretical result, although pleasing from the present point of view, is to a certain extent meaningless, as the value obtained for $\bar{D}_r$ in the Doi–Edwards theory depends strongly on the choice of the value of L. (This is due to the L^3 term in D_{r0}, in combination with the $(\nu L^3)^{-2}$ term in the expression for $\bar{D}_r$, leading to an L^{-7} dependence in all, at a constant weight fraction of polymer; see the equations in the Appendix.) If instead of the persistence length the contour length, which is a reasonable upper bound for L, is chosen, the Doi–Edwards rotation diffusion constant is $\approx 0.25\ s^{-1}$. Alternatively, if for L, as a lower bound, the deflection length L_d as introduced by Odijk[14] is chosen, the rotational diffusion constant is unreasonably high. (Using $L_d \equiv L_p/\alpha \approx L_p(1 - \langle P_2 \rangle)/3 = 0.5$ nm gives a negative value for D_{r0}, as $L < b$. Using the approximate expression $D_{r0} = 4k_BT/\pi\eta_s L^3$, $\bar{D}_r$ becomes $\approx 10^{16}\ s^{-1}$.)

The values of $\bar{D}_r$ given above show that, although it is perfectly reasonable to assume that external flows do strongly influence the degree of molecular orientational order with respect to the director, there is also an equally good case to be made for the slow-flow approximation in the high-concentration regime. Here the slow-flow approximation has been chosen, as it enormously simplifies the problem. In addition it is felt that the comparison of the slow-flow results with the experimental data on the fibre modulus is a reasonable test of the validity of the slow-flow approximation for concentrated aramid solutions. From the agreement of the present model with the experimental results it is concluded that it is possible to explain the observed influence of polymer concentration, coagulation bath temperature, and draw-down on the modulus of aramid fibres by using a combination of molecular orientational order with respect to the local director and affine deformation of the director field itself.

As regards the affine deformation model, it is conceded that the use of the pre-draw factor is somewhat ambiguous at present. However, the use of the affine deformation model to describe the effect of draw-down in the air gap seems acceptable. To test this part of the model experimentally, synchrotron X-ray scattering experiments in an elongational flow spinning geometry are planned for the near future.

It would seem worthwhile to try to take the affine deformation model further, viz. to other geometries, so as to be able to analyse the influence of the spinneret geometry. MacMillan[16] has analysed the stability of the director field under affine deformation for a variety of cases, including of course also the simple shear and elongation geometry. Unfortunately no expressions were given for the 'director order parameters', so the relation to mechanical properties cannot be established without some additional effort.

Considering the various approximations that are used, it may be wondered to what extent the present approach has any predictive power. It should be realized that in practice with a dry-jet wet spinning process, a draw ratio in the air gap of ≈ 6 or more will often be applied. For these $DR_{\text{air-gap}}$ values the fibre modulus is to a large extent determined by $\langle P_2 \rangle$. By simply combining equations (12), (20) and (21), a reasonable first-order estimate for the fibre modulus can be obtained that is often quite close to the experimental value (say within 20 GPa). This holds true not only in the concentrated regime, as described here, but also for much more dilute solutions close to the isotropic phase. As an example, a DABT solution spun at 9 wt% and 5°C leads to aramid fibres with a modulus of ≈ 35 GPa. Using equations (12), (20) and (21), a predicted modulus of 36.6 GPa is found. To use equations (12) for predicting the modulus of fibres spun from other lyotropic systems, only one experimental value for T_{ni} at given concentration has to be measured to calibrate the absolute temperature scale of the model.

ACKNOWLEDGEMENTS

The authors thank Professor H. N. W. Lekkerkerker and Dr J. J. van Aartsen for many useful discussions and their continued interest in this work, and Ing. B. Krins for assistance with the spinning experiments.

REFERENCES

1 Picken, S. J. *Macromolecules* 1989, **22**, 1766
2 Picken, S. J. *Macromolecules* 1990, **23**, 464
3 Northolt, M. G. and van der Hout, R. *Polymer* 1985, **26**, 310
4 Doi, M. and Edwards, S. F. 'The Theory of Polymer Dynamics', Clarendon Press, Oxford, 1986, pp. 289–380
5 Marucci, G. and Maffetone, P. L. *Macromolecules* 1989, **22**, 4076
6 Larson, R. G. *Macromolecules* 1990, **23**, 3983
7 Maier, W. and Saupe, A. *Z. Naturforsch.* 1959, **A14**, 882; 1960, **A15**, 287
8 Picken, S. J., Aerts, J., Visser, R. and Northolt, M. G. *Macromolecules* 1990, **23**, 3849
9 Vainshtein, B. K. 'Diffraction of X-rays by Chain Molecules', Elsevier, Amsterdam, 1966, pp. 274–281
10 Picken, S. J., Aerts, J., Doppert, H. L., Reuvers, A. J. and Northolt, M. G. *Macromolecules* 1991, **24**, 1366
11 Kuhn, W. and Grün, F. *Kolloid-Z.* 1942, **101**, 248
12 Viola, G. G. and Baird, D. G. *J. Rheol.* 1986, **30**, 601
13 Kenig, S. *Polymer Eng. Sci.* 1987, **27**, 887
15 Odijk, T. *Macromolecules* 1986, **19**, 2313
16 MacMillan, E. H. *J. Rheol.* 1989, **33**, 1071

APPENDIX

The Doi–Edwards rotational diffusion constant for concentrated solutions of rods is given by[4]

$$\bar{D}_r = \beta D_r^*(\nu^*/\nu)^2(1 - S^2)^{-2} = \beta D_{r0}(\nu L^3)^{-2}(1 - S^2)^{-2}$$

where v is the number fraction of rods of length L, S is the $\langle P_2 \rangle$ order parameter (at rest), β is a correction factor of the order of 10^3, and D_{r0} is the rotational diffusion constant for a dilute solution, given by

$$D_{r0} = \frac{3k_B T(\ln(L/b) - \gamma)}{\pi \eta_s L^3}$$

where L/b is the aspect ratio of the rod, γ is a correction term (≈ 0.8), η_s is the solvent viscosity (5.3 mPa s for 99%/80°C H_2SO_4), and T is the temperature. Using for the L the persistence length of 29 nm and $b = 0.66$ nm, $D_{r0} = 1.1 \times 10^5\ s^{-1}$. For a concentrated aramid solution with $\langle P_2 \rangle \approx 0.95$ (at rest), this gives $\bar{D}_r = 3.3 \times 10^4\ s^{-1}$.